



Crystallinity and optical properties of β -Ga₂O₃/Ga₂S₃ layered structure obtained by thermal annealing of Ga₂S₃ semiconductor

Veaceslav Sprincean^a, Oleg Lupan^{b,c,**}, Iuliana Caraman^d, Dumitru Untila^{a,d}, Vasile Postica^{c,1}, Ala Cojocaru^{e,1}, Anna Gapeeva^{b,1}, Leonid Palachi^f, Rainer Adeling^b, Ion Tiginyanu^{g,h,*}, Mihail Caraman^a

^a Faculty of Physics and Engineering, Moldova State University, 60 Alexei Mateevici Str., MD-2009, Chisinau, Republic of Moldova

^b Chair for Functional Nanomaterials, Faculty of Engineering, Institute for Materials Science, Kiel University, Kaiser Str. 2, D-24143, Kiel, Germany

^c Center for Nanotechnology and Nanosensors, Technical University of Moldova, 168 Stefan Cel Mare Av., MD-2004, Chisinau, Republic of Moldova

^d Institute of Electronic Engineering and Nanotechnology, Academiei Str. 3/3, MD-2028, Chisinau, Republic of Moldova

^e Phi-Stone AG, Kaiserstr. 2, D-24143, Kiel, Germany

^f Free International University of Moldova, ULIM, Str. Vlaicu Parcalab, 52, MD-2012, Chisinau, Republic of Moldova

^g National Center for Materials Study and Testing, Technical University of Moldova, Stefan Cel Mare Av. 168, MD-2004, Chisinau, Republic of Moldova

^h Academy of Sciences of Moldova, Stefan Cel Mare Av. 1, MD-2001, Chisinau, Republic of Moldova

ARTICLE INFO

Keywords:

Gallium oxide

β -Ga₂O₃/Ga₂S₃

Crystalline β -Ga₂S₃

Semiconductor

Scanning electron microscopy

ABSTRACT

In this work, the β -Ga₂O₃ nanostructures were obtained by thermal annealing in air of β -Ga₂S₃ single crystals at relatively high temperatures of 970 K, 1070 K and 1170 K for 6 h. The structural, morphological, chemical and optical properties of β -Ga₂O₃- β -Ga₂S₃ layered composites grown at different temperatures were investigated by means of X-ray diffraction (XRD), scanning electron microscopy (SEM), energy-dispersive X-ray spectroscopy (EDX) as well as photoluminescence spectroscopy (PL) and Raman spectroscopy. The results show that the properties of obtained β -Ga₂O₃- β -Ga₂S₃ composites were strongly influenced by the thermal annealing temperature. The XRD and Raman analyses confirmed the high crystalline quality of the formed β -Ga₂O₃ nanostructures. The absorption edge of the oxide is due to direct optical transitions. The optical bandwidth was estimated to be approximately 4.34-4.41 eV, depending on the annealing temperature. Annealing of the β -Ga₂S₃ monocrystals at a higher temperature of 1170 K showed the complete conversion of the surface to β -Ga₂O₃. These results demonstrate the possibility to grow high quality β -Ga₂O₃- β -Ga₂S₃ layered composites and β -Ga₂O₃ nanostructures in large quantities for various applications such as gas sensing, non-toxic biomedical imaging, nonlinear optical, as well as power device applications. Micro and nanocrystallites present on the surface of the Ga₂O₃ layer contribute to a diffusion of the incident light which leads to an increase of the absorption rate allowing thus to reduce the thickness of the Ga₂O₃ layer, in which the generation of unbalanced charge carriers takes place. By decreasing the Ga₂O₃ layer thickness in such layered composites, the efficiency of photovoltaic cells based on such junctions can be increased.

1. Introduction

Monoclinic gallium oxide (β -Ga₂O₃) is an important semiconductor compound with high chemical and thermal stability as well as a wide bandgap of 4.5 – 4.9 eV, which is the widest energy gap among the transparent conducting oxides [1–4]. Therefore, β -Ga₂O₃ is an attractive material for optoelectronic applications, especially for a solar-blind

high-temperature deep-ultraviolet photodetector [5–8]. Since it possesses a band gap wider than In₂O₃, and it is optically transparent in the UV-NIR spectral range β -Ga₂O₃ is a good electrically conductive and transparent optical electrode for optoelectronic and photovoltaic devices [9,10]. For example, Kong et al. fabricated a graphene- β -Ga₂O₃ heterojunction for highly sensitive deep UV (254 nm) photodetector application with a high external quantum efficiency, very good stability

* Corresponding author. , National Center for Materials Study and Testing, Technical University of Moldova, Republic of Moldova.

** Corresponding author. Institute for Materials Science, Kiel University, Germany.

E-mail addresses: ollu@tf.uni-kiel.de, oleg.lupan@mib.utm.md, lupan@physics.ucf.edu (O. Lupan), ion.tigineanu@cstm.utm.md (I. Tiginyanu).

¹ These authors contributed equally.

and reproducibility [11]. Zhong et al. fabricated UV photodetectors based on high quality β -Ga₂O₃ single crystals, synthesized via chemical vapour deposition (CVD) method showing excellent optoelectronic performance with high sensitivity, fast response speed, excellent stability and reversibility [2]. Chen et al. fabricated a strain modulated solar-blinded photodetector based on ZnO-Ga₂O₃ core-shell heterojunction microwire which demonstrated high sensitivity to deep UV light centred at 261 nm [12]. Among other applications of Ga₂O₃ nanostructures one can mention high-temperature humidity and gas sensors [13–15], solar blind UV radiation detectors [11,16,17], photocatalytic splitting of water and electrochemical hydrogen generators [18]. Versatile applications of Ga₂O₃ are possible due to its high structural stability at elevated temperatures, and a large potential for real gas sensing applications in harsh environments [8,14,19,20].

Currently, there are several technological approaches to obtain Ga₂O₃ nanocrystals with different morphologies such as nanowires, nanoribbons, nanospheres, nanorods and others [3,17,21–25]. β -Ga₂O₃ nanostructures can be synthesized by thermal oxidation of metallic Ga in the N₂/O₂ atmosphere of the GaN and GaAs composites as well as gallium chalcogenides (GaSe, GaS, Ga₂S₃) [18,23,26]. In the previous work [27], a Ga₂O₃ layer in the form of needles was grown by surface oxidation of a Zn-doped GaAs plate. The GaAs:Zn plates were annealed at $T = 1320$ K for 40 min in atmosphere of O₂-Ar. The mechanism of formation of Ga₂O₃ needles on the surface of GaSe and GaS plates by thermal annealing in atmosphere in the temperature range from 998 to 1200 K was studied in previous works [23,28]. In the case of thermal annealing in the flux of a O₂-NH₃ solution, the GaSe surface was covered with porous micro-structures similar to flowers [29]. Such structures exhibit photocatalytic activity superior to TiO₂ oxide, which are widely used in chemical technologies [28]. A thorough knowledge of the basic structural, optical and vibrational properties of β -Ga₂O₃- β -Ga₂S₃ is needed since information on composites structure is still lacking. β -Ga₂O₃- β -Ga₂S₃ composites are important for fundamental research as well as for various applications including sensors for harsh environments, non-toxic biomedical imaging, energy down-conversion in nanostructured solar cells, nonlinear optical applications, optoelectronic devices, e.g., high-power laser radiation sensors [8,14,15,19,30]. In the case of β -Ga₂O₃- β -Ga₂S₃ composite, due to the p -type conductivity of Ga₂S₃ [31] and n -type conductivity of the Ga₂O₃ [32], formed p - n heterojunctions at the interface of β -Ga₂O₃- β -Ga₂S₃ are very attractive for gas sensing applications and UV photodetectors [33], in terms of enhanced gas sensing properties and increased efficiency of photo-generated electrons and holes separation [34]. So far, however, the sensing properties of the β -Ga₂O₃- β -Ga₂S₃ composite have not been investigated. Therefore, this composite is highly attractive for sensing applications, especially in harsh environments where other materials can't survive.

In this work, the crystalline structures of β -Ga₂O₃- β -Ga₂S₃ composites were successfully synthesized using a simple method of thermal oxidation in ambient air. The thermal annealing of β -Ga₂S₃ single crystals was performed at different temperatures and β -Ga₂O₃- β -Ga₂S₃ composites were grown. The surface morphology, structural, chemical and optical properties are reported and discussed in details.

2. Experimental part

The β -Ga₂O₃- β -Ga₂S₃ layered composites and Ga₂O₃ nanocrystals were obtained by the post-growth conversion of Ga₂S₃ single crystals shaped as plates, which were grown by chemical vapour deposition (CVD) using I₂ vapour as a carrier gas. Elemental components Ga (5 N) and S (5 N), taken in stoichiometric amounts by precision weighing (10⁻⁴ g), were used to obtain single crystals of Ga₂S₃. The experimental apparatus and the temperature profile of the two-section furnace used for growth of Ga₂S₃ crystals are presented in Fig. 1. By using the Bridgman–Stockbarger method a polycrystalline ingot with a mass of ~ 20 g was grown (see Fig. 2(a)). The Bridgman–Stockbarger method

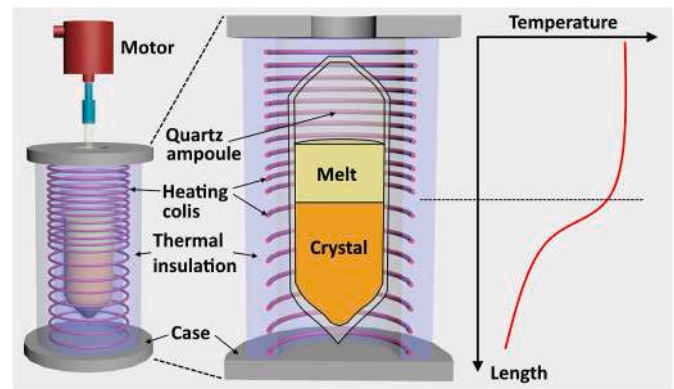


Fig. 1. Experimental apparatus and temperature profile of two-section furnace used for growth of polycrystalline ingot by Bridgman–Stockbarger method.

(VBS) is widely used for bulk crystal growth due to its comparative simplicity [35]. In this case, a regime of convection in the fluid phase is likely to be the major factor which controls radial and axial segregation in the growing crystal and is mainly affected by thermal conditions [35]. Quantities of Ga and S were placed in the quartz containers with internal diameter of ~ 20 mm, length of ~ 20 cm and wall thickness of 3 mm. Initially, the quartz container was treated for 40 min with hydrofluoric acid and then washed with bi-distilled water followed by drying at 200 ÷ 250 °C in a furnace. The synthesis of the compound was conducted in the two-section furnace with different temperatures. Ga was located in the temperature region at ~ 1400 K, while S was placed in the temperature region of ~ 750 K. S vapour at this temperature did not exceed 2 atm [36]. Sulphur was separated from the area where Ga was placed with a recess in the wall of the container. The furnace was tilted at ~ 15° from the horizontal. During the synthesis process, the container was rotated around the axis at ~ 2 rpm (240 π rad/h). As a result of Ga₂S₃ formation the amount of S from the cold zone of the furnace is reduced over time. After the reaction of S from lower temperature region with Ga, the temperature along the container was established to ~ 1400 K. At this temperature, the melt was mixed and homogenized by vibrating the container with a frequency of ~ 50 Hz for 4 h, after which the furnace temperature was decreased to ~ 700 K with a fixed rate of ~ 100 °C/h, followed by switching off the furnace and allowing the Ga₂S₃ ingot to cool down naturally to room temperature inside of the furnace for 12 h.

For the synthesis of Ga₂S₃ single crystals ~ 10 g of the obtained ingot material and 2 mg/cm³ of I₂ were placed into a quartz vial with a diameter of ~ 20 mm and a length of 18–20 cm. Prior to the thermal treatment, the quartz vial was evacuated to 5·10⁻⁵ torr, followed by sealing of the container and introduction into the two-section horizontal furnace. One region with a temperature of 1020 K represents the source zone, while the second region with 990 K represents the crystallization zone. The synthesis process takes approximately 120 h. In Fig. 2(b), an optical image of Ga₂S₃ single crystals is depicted.

For obtaining of Ga₂O₃-Ga₂S₃ layered structures plate-shaped Ga₂S₃ single crystals with thickness of about 3–8 mm were choose. The electrical conductivity of plate-shaped Ga₂S₃ single crystals at room temperature was (2.5 ÷ 3.0)·10⁻¹² Ω^{-1} cm⁻¹. Selected monocrystals were subjected to thermal annealing at 970 K–1170 K for 3–6 h in ambient air which resulted after thermal annealing in the formation of a white layer on the surface of the samples. The electrical conductivity of the surface layer was investigated in four sample sets with thickness values of 3.2, 3.9, 4.5 and 6.8 mm and amounted to (4 ÷ 5)·10⁻⁹ Ω^{-1} cm⁻¹. One of the sample surfaces was sanded to half the thickness so that a characteristic colour of the primary material (Ga₂S₃) was obtained. The electrical conductivity on the surface of this layer for the studied samples was (1.5 ÷ 2.0)·10⁻⁸ Ω^{-1} cm⁻¹. In order to verify that the exposed layer indeed consisted of the primary crystal (Ga₂S₃), the photoluminescence (PL) spectrum of the untreated Ga₂S₃ single crystal was compared to the

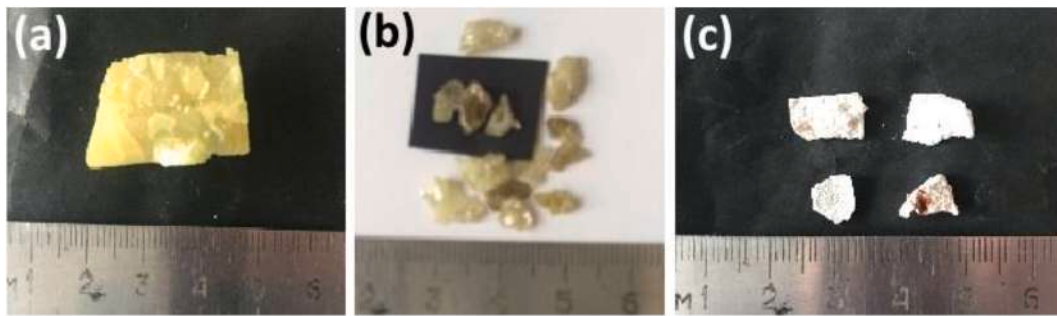


Fig. 2. Optical images of Ga₂S₃ crystals: (a) grown by Bridgman–Stockbarger method using Ga and S taken in stoichiometric amounts; (b) monocrystals grown by CVD with I₂; (c) materials obtained after thermal annealing of Ga₂S₃ in ambient air at a temperature of 1170 K for 6 h.

spectrum of the polished Ga₂O₃-Ga₂S₃ sample. Both PL spectra from the primary crystals and from the surface of the polished sample represents a band in the red region of the spectrum with a maximum at ~ 680 nm, which confirmed the chemical compounds were identical. In Fig. 2(b) and (c) typical samples of the initial Ga₂S₃ single crystals as well as nanostructures after thermal annealing in the ambient air at 1170 K for 6 h are depicted, respectively. The surface morphology of the synthesized samples was studied using the scanning electron microscope (SEM), the Zeiss Ultra Plus type, equipped with an EDX analysis system from Oxford Instruments [37]. The structural properties were investigated by X-ray diffraction technique (XRD) using a Rigaku Ultima IV diffractometer (CuK α radiation, $\lambda = 1.5406 \text{ \AA}$, 40 kV to 40 mA) in Bragg-Brentano geometry (θ - 2θ) with a fixed X-ray tube. The combined diffusion spectra were recorded using a WITec alpha300 Raman spectrometer. All micro-Raman spectra were taken with the help of WITec RA300 microscope (the excitation light, 532 nm), to identify the phase of materials as described in previous papers [25,38].

Absorption edge of the oxide layers, formed on the surface of Ga₂S₃ crystals, was investigated by measuring the diffuse reflection coefficient (R_d) using a spectral spectrophotometer M – 40, equipped with an accessory for recording the diffuse reflection spectrum in the 200–900 nm spectral range. Absorbance of the oxide layer was determined using Kubelka – Munk (K-M) function, $F(R_d)$ [39,40]:

$$F(R_d) \frac{(1 - R_d)^2}{2R_d} = \frac{\alpha}{S} \quad (1)$$

where α is absorbance coefficient and S is the scattering factor. Photoluminescence spectra of the Ga₂S₃ and Ga₂O₃/Ga₂S₃ crystals were measured using a setup based on a high optical power monochromator MDR-2, equipped with the profiled diffraction grids of 1200 mm⁻¹ and 600 mm⁻¹ and based on photomultiplier with (Na₂K)Sb + Cs photocathode with selective amplifier. The excitation wavelength was 255 nm, selected from the excitation beam band of the emission spectra for Xe lamp (1000 W) using a ZMR-3 monochromator with a quartz prism. The PL spectra of Ga₂S₃ single crystals measured at 80 K was excited using a N₂ laser ($\lambda = 337 \text{ nm}$ and average power of 20 mW).

3. Results and discussion

3.1. Structural properties of layered Ga₂O₃-Ga₂S₃ composites

As can be observed from Fig. 2(b) and (c) the surface colour of Ga₂S₃ crystals is changed to white after thermal annealing at 1075 K for 4 h and crystals spread well the incident light. Ga₂S₃ single crystals with hexagonal crystalline lattice (α -Ga₂S₃), stable at a relatively low temperature ($T < 930 \text{ K}$), as well as monoclinic crystalline lattice (β -Ga₂S₃), stable up to the melting point, can be synthesized using the CVD method. For synthesis of Ga₂O₃-Ga₂S₃ composite structures the Ga₂S₃ crystals with monoclinic crystalline lattice were chosen. The XRD patterns of Ga₂S₃ crystals synthesized using the CVD method in I₂ vapour

atmosphere before and after thermal annealing are presented in Fig. 3 (curve *a* and *b*, respectively). All diffraction peaks were identified using PDF 01-071-2672 and included in Table 1, column BT. All the detected peaks in case of Ga₂S₃ crystals, used for synthesis of Ga₂O₃ on the Ga₂S₃ substrate, can be assigned to monoclinic β -Ga₂S₃ with following lattice parameters: $a = 11.107 \text{ \AA}$, $b = 6.395 \text{ \AA}$, $c = 7.021 \text{ \AA}$, $\alpha = 90.00^\circ$ and $\beta = 121.17^\circ$. The characteristic doublet of diffraction peaks for β -Ga₂S₃ at 2θ between 27° and 30° ($27^\circ < 2\theta < 30^\circ$) can be observed in Fig. 3(b) [41]. This doublet appears in XRD patterns measured for submicrometer β -Ga₂S₃ crystals grown in the form of cones, prisms, etc. [42].

In the case of XRD pattern measured for thermally annealed Ga₂S₃ crystallite in air at 1075 K for 4 h (see Fig. 3, curve 2) the detected peaks were assigned to monoclinic β -Ga₂S₃ (PDF #01-071-2672) and monoclinic β -Ga₂O₃ (PDF #01-087-1901) with lattice parameters: $a = 12.2 \text{ \AA}$, $b = 3.0 \text{ \AA}$, $c = 5.8 \text{ \AA}$, $\alpha = 90.00^\circ$, $\beta = 104^\circ$ and $\gamma = 90^\circ$. The information about diffraction peaks is included in Table 1, column AT. Because the position of some reflections of β -Ga₂S₃ and β -Ga₂O₃ are quite identical, it is difficult to clearly distinguish between the different crystalline phases. However, the clear evidence of β -Ga₂O₃ formation after thermal annealing can be observed at 2θ values from 30° to 40° (see Fig. 3(b)).

The concentration of Ga₂O₃ in Ga₂O₃-Ga₂S₃ composite structure can be increased by thermal annealing of smaller Ga₂S₃ crystals or by increasing the duration of thermal annealing at 1070 K. In the case of thermal annealing of Ga₂S₃ crystals with a diameter smaller than 4 μm for 6 h only the β -Ga₂O₃ phase can be obtained, without detection of Ga₂S₃. The XRD reflections with double components from region of 2θ equal to 31° , 38° , 42° , 54° , 58° and 76° are characteristic for β -Ga₂O₃ nanowires [7]. The small values of full width at half maximum (FWHM) of reflections from XRD pattern in the case of Ga₂O₃-Ga₂S₃ composites indicate a small diameter of crystals.

The crystallites diameters d of Ga₂S₃ and β -Ga₂O₃ from composites were estimated using the Debye-Scherrer equation [43]:

$$d = \frac{k\lambda}{FWHM \cos \theta_{hkl}} \quad (2)$$

where k is the Scherrer constant equal to 0.94, λ is the X-ray wavelength and θ_{hkl} is the Bragg diffraction angle. The crystallites diameter of 520 \AA for β -Ga₂S₃ was estimated using the reflection at 28.86° , while for β -Ga₂O₃ the value of 616 \AA was estimated using the reflection at 35.29° . Therefore, it can be assumed that during the conversion of the β -Ga₂S₃ crystal surface to β -Ga₂O₃ the formed oxide layer is nanostructured. The presence of other phases of Ga₂S₃ and Ga₂O₃ oxides has not been observed.

3.2. Morphological analysis of Ga₂O₃ layer on Ga₂S₃ substrate

In Fig. 4, SEM micrographs of un-treated and thermally annealed Ga₂S₃ crystals are depicted. From Fig. 4(a) and Figure S2(a) it can be observed that sliced Ga₂S₃ ingot, grown using Bridgman method, is composed of randomly oriented crystallites with a mean diameter of

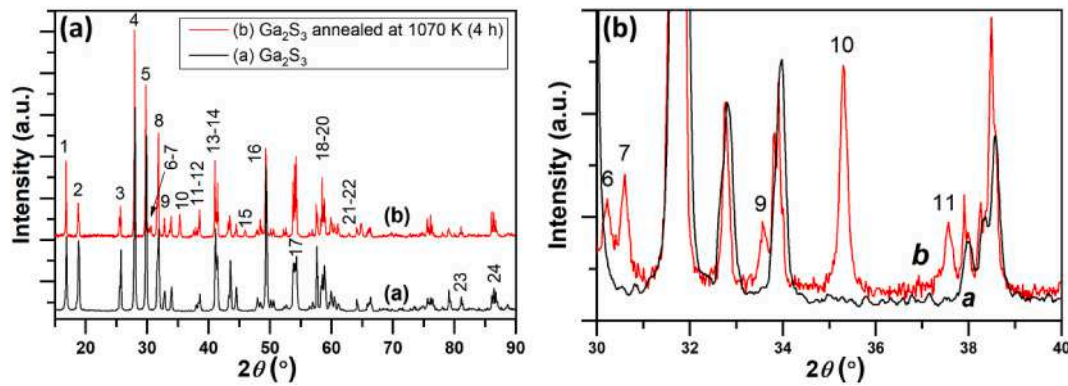


Fig. 3. (a) XRD patterns of the Ga_2S_3 crystals before thermal annealing (curve *a* in black) and after thermal annealing in air at 1070 K for 4 h (curve *b* in red). (b) Zoomed view of the peaks in the interval from 30 to 40°.

Table 1

Interpretation of reflections from XRD patterns measured for Ga_2S_3 crystals: before thermal annealing in air (BT) and after treatment (AT), at 1070 K for 4 h.

No.	Experimental values		Cards				
	BT	AT	Phase	PDF card #	2θ (°)	I, a. u.	<i>h k l</i>
1	16.86	16.78	Ga_2S_3	01-071-2672	16.70	61.4	1 1 0
2	18.84	18.76	Ga_2S_3	01-071-2672	18.66	40.5	2 0 0
3	25.70	25.63	Ga_2S_3	01-071-2672	25.58	17.9	-2 0 2
4	28.00	27.90	Ga_2S_3	01-071-2672	27.82	100.0	0 2 0
5	29.86	29.77	Ga_2S_3	01-071-2672	29.72	75.9	0 0 2
6		30.17	Ga_2O_3	01-087-1901	30.12	45.6	4 0 0
7		30.59	Ga_2O_3	01-087-1901	30.51	56.0	-4 0 1
8	31.86	31.74	Ga_2S_3	01-071-2672	31.76	33.2	0 2 1
9		33.56	Ga_2O_3	01-087-1901	33.49	25.3	-1 1 1
10		35.29	Ga_2O_3	01-087-1901	35.22	100	1 1 1
11		37.56	Ga_2O_3	01-087-1901	37.48	34.8	4 0 1
12	38.58	38.48	Ga_2S_3	01-071-2672	38.44	6.9	1 1 2
13	41.08	40.99	Ga_2S_3	01-071-2672	40.95	29.4	2 2 1
14	41.44	41.44	Ga_2S_3	01-071-2672	41.37	12.7	-3 1 3
15		45.87	Ga_2O_3	01-087-1901	45.84	21.5	-3 1 2
16	49.36	49.30	Ga_2S_3	01-071-2672	49.29	53.8	-3 3 1
17	54.04	53.99	Ga_2S_3	01-071-2672	53.99	24.9	0 2 3
18	57.58	57.60	Ga_2S_3	01-071-2672	57.61	4.4	0 4 0
			Ga_2O_3	01-087-1901	57.66	25.7	-3 1 3
19	58.82	58.78	Ga_2S_3	01-071-2672	58.78	15.6	-3 3 3
20	59.90	59.84	Ga_2S_3	01-071-2672	59.85	7.6	5 1 1
21		62.77	Ga_2O_3	01-087-1901	62.74	11.4	7 1 0
22		64.76	Ga_2O_3	01-087-1901	64.71	33.4	-7 1 2
23	81.10	81.02	Ga_2S_3	01-071-2672	81.07	3.0	3 5 0
			Ga_2O_3	01-087-1901	81.01	0.1	10 0 0
24	86.40	86.36	Ga_2S_3	01-071-2672	86.45	5.0	6 4 0
			Ga_2O_3	01-087-1901	86.35	1.3	0 0 5

about 5 μm . Using the CVD method with I_2 vapour as carrier gas, optically transparent single crystals with smooth surfaces were obtained. In Fig. 4(b), SEM micrographs of the Ga_2S_3 single crystal surface, grown using the CVD method, is depicted showing the single crystals growing directions. Therefore, it can be concluded that $\beta\text{-Ga}_2\text{S}_3$ single crystals possess a layered structure.

The SEM images of $\beta\text{-Ga}_2\text{S}_3$ single crystals thermally annealed at 970 K, 1070 K and 1170 K for 6 h are presented in Fig. 4(b-d) and Figure S2 (b-d), respectively. As can be observed, the surface of single crystals is nanostructured after thermal treatment. On the surface of the sample treated at 970 K (Fig. 4(b)) mainly two types of nanograins can be observed, namely the island-type with a contour of an indefinite form with a higher density and circular-shaped nanograins with a lower density. Both types of nanograins have a diameter of 10–100 nm. The Ga_2O_3 single crystal is known to show five polymorphs: $\alpha\text{-Ga}_2\text{O}_3$ with a corundum structure, monoclinic $\beta\text{-Ga}_2\text{O}_3$, cubic $\gamma\text{-Ga}_2\text{O}_3$ with a defective-spinel structure, $\delta\text{-Ga}_2\text{O}_3$ and $\varepsilon\text{-Ga}_2\text{O}_3$ [44], having different

surface properties [45,46]. For these reasons, at least two phases of the gallium oxide are formed on the surface of the Ga_2S_3 single crystals. From the analysis of XRD diagrams the presence of the monoclinic $\beta\text{-Ga}_2\text{O}_3$ phase is well established. The β phase belongs to $C2/m$ space group and is known to be the most stable structure among others, which is formed at high growth temperatures as in our case, while the other phases are meta-stable [3]. Once it is formed, it is highly stable at all temperatures below the melting point (~ 1800 °C) of $\beta\text{-Ga}_2\text{O}_3$ [15,30].

Thermally annealed Ga_2S_3 crystals at higher temperature of 1070 K showed no essential changes in the morphology of the samples compared to treatment at 970 K (see Fig. 4(c) and S2(c)). At this temperature the area of islands on the surface of Ga_2S_3 crystals is increasing up to tens of μm^2 . In Fig. 4(d) and Figure S2(d) the SEM image of the Ga_2S_3 crystal thermally annealed at 1170 K is presented. The surface of the crystal is perpendicular to the *b*-axis. As can be observed, the area of the formed $\beta\text{-Ga}_2\text{O}_3$ crystals is increased by the formation of networks of islands on the surface of Ga_2S_3 . Ga_2O_3 crystallites with a parallelogram shape and fragments with weakly outlined edges were obtained on a GaAs substrate using the CVD method in an atmosphere of N_2/O_2 [47].

3.3. Selected area energy dispersive X-ray spectroscopy (EDX)

The chemical composition of the $\text{Ga}_2\text{O}_3\text{-Ga}_2\text{S}_3$ composites obtained by thermal annealing at 970 K, 1070 K and 1170 K for 6 h was investigated using EDX equipped at SEM. The EDX spectra of the samples are presented in Supporting Information, Figure S1. Insets show SEM images of the respective sample and region where the spectrum was measured. The content of Ga, O and S elements in $\text{Ga}_2\text{O}_3\text{-Ga}_2\text{S}_3$ composites is presented in Table 2 and in insets of Figure S1, showing the decrease in content of S with the increasing treatment temperature from 970 K to 1070 K. Generally, the content of S in all treated samples is relatively small, i.e. about 0.19, 0.05 and 0.00 at% for samples treated at 970 K, 1070 K and 1170 K, respectively. Therefore, it can be concluded that by annealing at a temperature higher than 1170 K the content of S can be totally excluded from the surface of the crystal, i.e. only a layer of Ga_2O_3 nanocrystals is formed with the Ga:O atomic ratio of $\sim 2/3$, which is in a good agreement with the nominal stoichiometric composition of Ga_2O_3 .

3.4. Raman spectroscopy of $\text{Ga}_2\text{O}_3\text{-Ga}_2\text{S}_3$ composites

Micro-Raman spectroscopy is a very sensitive technique for the investigation of surface properties of composite materials [25,48–50]. Fig. 5 shows the room temperature Raman spectra of the Ga_2S_3 crystals treated in air at 970 K (see Fig. 5(a)) and 1070 K (see Fig. 5(b)) for 6 h. All detected peaks of the $\text{Ga}_2\text{O}_3\text{-Ga}_2\text{S}_3$ composites are assigned in Table 3. As can be observed, no peaks corresponding to $\beta\text{-Ga}_2\text{S}_3$ phase are observed on the surface of the thermally annealed $\beta\text{-Ga}_2\text{S}_3$ crystals at 1070 K and 1170 K. Therefore, the surface of $\beta\text{-Ga}_2\text{S}_3$ crystals is totally

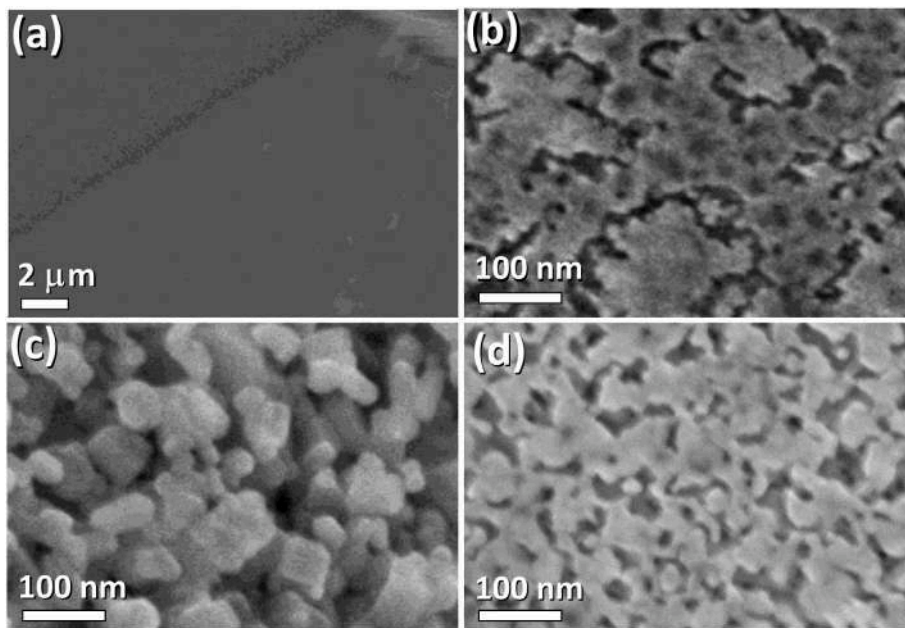


Fig. 4. SEM images of (a) pristine Ga₂S₃ crystals and Ga₂S₃ crystals after thermal annealing for 6 h at following temperatures: (b) 970 K; (c) 1070 K; and (d) 1170 K.

Table 2

Content of O, S and Ga in the Ga₂O₃-Ga₂S₃ composites.

Element	Content, at%		
	970 K	1070 K	1170 K
O	59.81	66.18	59.51
S	0.19	0.06	0.00
Ga	40.00	33.76	40.49
Total	100.00	100.00	100.00

converted to β-Ga₂O₃ with C_{2h}³ (C2/m) symmetry group [25,51,52]. The 10 atoms based primitive unit cell of β-Ga₂O₃ produces 30 phonon modes, including 27 optical modes [15,30]. These optical phonon modes of β-Ga₂O₃ at the Γ point in the Brillouin zone are classified as follows [51–53]:

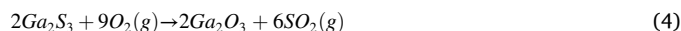
$$\Gamma_{opt} = 10A_g + 5B_g + 8B_u + 4A_u \quad (3)$$

from which 15 modes are Raman active (10A_g + 5B_g) and those with odd parity, namely (4A_u + 8B_u), 12 modes are infrared active [51,54]. For comparison purposes the wavenumber (cm⁻¹) of Raman active modes for α-Ga₂S₃ are also included, as well as symmetry and wavenumber of Raman active modes for β-Ga₂O₃ [51].

Thus, we can conclude that the surface of β-Ga₂S₃ crystals annealed

at 1070 K and 1170 K in air is completely covered with a homogeneous layer of β-Ga₂O₃. The thickness of this layer is enough to spread the laser radiation with the wavelength 532 nm, used as excitation source. Also, from Fig. 5 it can be seen that an increase in the annealing temperature from 1070 K to 1170 K leads to an increase in the intensity of the peaks at 346.2 cm⁻¹ and 629.4 cm⁻¹, a similar phenomenon being observed in the case of β-Ga₂O₃ nanowires, nanobelts, nanoblades grown by various technological processes [55–58].

The tentative reaction of β-Ga₂S₃ conversion into β-Ga₂O₃ in the presence of oxygen molecules from ambient air can be described as follows [59]:



Therefore, the formation of nanostructured layers of β-Ga₂O₃ on the surface of β-Ga₂S₃ single crystals can be the result of S evaporation as SO₂ gas. For example, Li et al. observed that oxidation of single crystalline ZnS nanobelts results in conversion to ZnO nanotwin belts with the formation of nanovoids in the central part along the length direction [59].

Lattice dynamical properties of the β-Ga₂O₃ are well investigated by first principles in Ref. [60], where all peaks in a wavenumber interval from 160 to 420 cm⁻¹ are considered as non-degenerated symmetrical A_g vibrational modes. The dominant mode at 199.6 cm⁻¹ is interpreted as the mode of vibration and translation of the assemblies of atoms

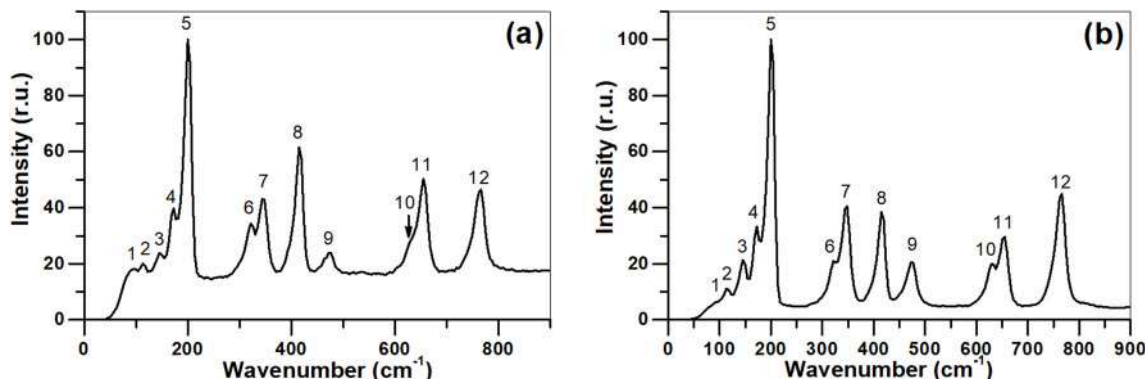


Fig. 5. Room temperature micro-Raman spectra of the β-Ga₂S₃ monocrystals thermally annealed in air for 6 h at: (a) 1070 K; and (b) 1170 K.

Table 3

Wavenumbers assigned to peaks detected in Raman spectra of β -Ga₂S₃ crystals measured at the excitation wavelength of 532 nm (0.1 W) and of the thermally annealed β -Ga₂S₃ monocrystals for 6 h at 1070 K and 1170 K.

No.	β -Ga ₂ S ₃ (untreated)		β -Ga ₂ S ₃ (thermally annealed)				β -Ga ₂ O ₃ [51]	
	$\bar{\nu}$, cm ⁻¹	<i>I</i> , a. u.	1070K		1170K		Mode [51]	Frequency ν cm ⁻¹
			$\bar{\nu}$, cm ⁻¹	<i>I</i> , a. u.	$\bar{\nu}$, cm ⁻¹	<i>I</i> , a. u.		
1	67.5	19.0	94.1	247.3	94.76	135.3		
2	84.0	9.9	114.2	273.2	115.2	235.0	B _g	113.6
3	116.6	15.2	145.7	323.4	145.7	452.3	B _g	144.7
4	141.7	11.3	171.6	540.7	171.6	705.4	A _g	169.2
5	147.9	26.8	199.6	1358.4	199.6	2014.0	A _g	200.4
6	228.4	100.0	322.3	466.5	321.3	441.3	A _g	318.6
7	302.4	18.0	345.9	585.6	346.2	831.8	A _g	346.4
8	327.4	22.0	415.8	836.2	414.8	812.1	A _g	415.7
9	386.4	30.8	475.5	325.6	475.5	431.3	B _g	473.5
10			627.7	378.5	629.4	421.5	B _g	628.7
11			655.6	683.8	654.6	625.7	A _g	652.5
12			766.0	631.5	766.0	949.0	A _g	763.9

arranged in the tetrahedron and octahedron configuration, while vibrational modes situated in a wavenumber interval of 600–700 cm⁻¹ are associated with the extension and contacting of GaO₄ tetrahedrons [54,61].

3.5. Optical properties of Ga₂O₃ layer on Ga₂S₃ substrate

Diffuse reflection spectra (R_d) of the Ga₂S₃ single crystals thermally annealed in air at 970 K, 1070 K and 1170 K were measured for wavelengths in the range of 230–450 nm. The spectral dependence of absorbance (α/S) was determined using K-M function (see equation (1)). The results are plotted in Fig. 6. As can be observed, the absorbance dependence on wavelength in the region of the absorption band edge has two main regions, namely a region of 360–300 nm with a slow change of absorbance and a region with a fast change at $\lambda < 290$ nm ($h\nu = 4.28$ eV). The second region represents the absorption edge, typical for the β -Ga₂O₃, grown by chemical methods [39]. Du Xuejian et al. observed the red-shift of the absorption edge for β -Ga₂O₃ nanostructures by doping it with Sn [62]. As can be observed from the inset in Fig. 6, the absorption edge can be well described with two linear sections of $[F(R_d)(h\nu)]^2 = A(h\nu - D)$ function, which is typical for direct bandgap transitions.

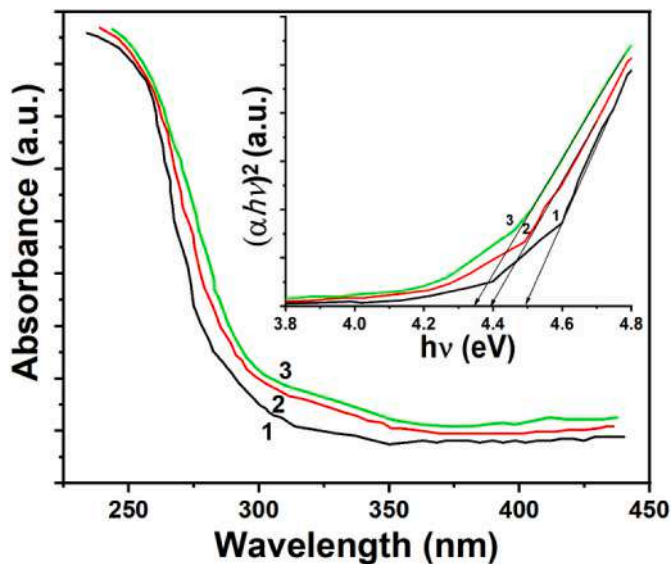


Fig. 6. Absorption spectra of layered structure of β -Ga₂O₃/Ga₂S₃ crystals annealed in air at: 970 K (curve 1); 1070 K (curve 2); and 1170 K (curve 3). In the inset the plot of $(\alpha h\nu)^2$ vs. photon energy ($h\nu$) is presented.

At the photon energy ($h\nu$) higher than 4.8 eV the experimental data of curve (2) fit very well a line with the edge at 4.8 eV. Zhengwei et al. demonstrated that the dimensions, type and bandgap of β -Ga₂O₃ nanostructures depend on the growth temperature [63]. Experimental results from Fig. 6 indicate that the direct band gap of the β -Ga₂O₃ nanocrystals tends to shrink with increasing annealing temperature of Ga₂S₃ single crystals near to the melting point. The optical bandgap was obtained from the intercept of $(\alpha h\nu)^2$ vs. photon energy ($h\nu$) (see inset in Fig. 6). The optical bandgap values for samples treated at 970 K, 1070 K and 1170 K are 4.50 eV, 4.41 eV and 4.34 eV, respectively. These values are similar with those reported in other works for nanostructures of β -Ga₂O₃ [39,62].

The decrease of optical bandgap values with increasing annealing temperature of Ga₂S₃ single crystals can be caused by the variation of oxygen vacancy concentration in the samples. It was demonstrated that the bandgap value depends on the dimensions of Ga₂O₃ crystallites and on the substrate type [56,64,65].

The room temperature PL spectra of Ga₂S₃ single crystals annealed at 970 K (curve 1), 1070 K (curve 2), 1170 K (curve 3) are presented in Fig. 7. The PL spectrum covers the wavelength range from 355 nm to 610 nm. As can be observed, the contour of the PL spectrum depends on

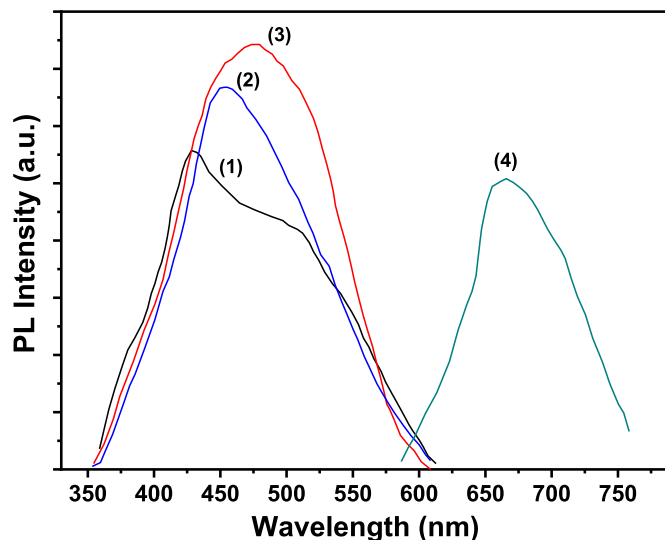


Fig. 7. Room temperature PL spectra of the layered structure of β -Ga₂O₃/Ga₂S₃ crystals obtained from Ga₂S₃ monocrystals annealed in air for 6 h at: 970 K (1); 1070 K (2); 1170 K (3) at the excitation wavelength of $\lambda = 250$ nm, and PL spectrum of Ga₂S₃ monocrystal (4) at the excitation wavelength of $\lambda = 337.4$ nm (~ 60 mW).

the annealing temperature of the Ga₂S₃ single crystals. At annealing temperature of 970 K the PL spectra are composed of at least three subbands, one well contoured that shows a broad peak at 428 nm (2.90 eV) and two steps at 380 nm (3.26 eV) and at 503 nm (2.46 eV). With an increase of annealing temperature by ~ 100 °C (1070 K) the PL spectrum is transformed into a curve with a maximum at 452 nm (2.74 eV). Further increase of the annealing temperature to 1170 K leads to a shift of the peak maximum to larger wavelengths of the PL spectrum. At this annealing temperature the maximum peak position is at 476 nm (2.60 eV).

As can be seen in the SEM images, the annealing temperature of the Ga₂S₃ single crystals determines the surface morphology of the oxide layer. Also, the edge of the fundamental absorption band depends on the oxidation temperature. Thus, we can admit that the PL spectra also depend on the type of micro and nanostructures (wires, bands, ropes, pyramid trunks) and the distribution on their surface. Ho et al. studied the PL spectra of Ga₂O₃ nanoribbons at room temperature [26]. The PL spectrum of these nanostructures covers the range 390 ÷ 550 nm and contains two main peaks at 418 nm and 439 nm. Also, it was demonstrated that emissions in PL spectra do not depend on the polymorph of Ga₂O₃, and for α , β and γ - Ga₂O₃ the main peak is centred in the 485 ÷ 500 nm region [66]. The maximum PL band of Ga₂O₃ nanobelts in Ref. [67] is found at the wavelength of 460 nm. Thus, it can conclude that the Ga₂O₃ oxide layer on the Ga₂S₃ substrate is composed of different types of nano-formations. Thus, at the annealing temperature of 973 K nanowires are predominating morphology while at 1173 K the oxide layer consists of nanobelts. In Fig. 7 (curve 4) the room temperature PL spectra of Ga₂S₃ single crystals are presented for comparison (curve 4). The PL spectrum of curve 4 is localized in the red region of wavelengths higher than 600 nm. The absence of PL emission of annealed samples in the red region of the spectrum indicates that the homogeneous structure of the Ga₂O₃ oxide layer is formed during the thermal annealing of Ga₂S₃ crystals in atmosphere. The PL spectra of the β -Ga₂O₃/ β -Ga₂S₃ heterostructure with a nanostructured Ga₂O₃ layer on top show two emissions at 420 nm and at wavelengths higher than 600 nm, with the maximum peak intensity at ~ 690 nm [68]. Thus, we can conclude that the presence of impurities in Ga₂S₃, especially in the composite obtained at the annealing temperature of 970 K, does not influence the structure of the PL spectrum.

3.6. Potential semiconducting applications of Ga₂O₃ layer on Ga₂S₃ substrate

β -Ga₂O₃ has been widely used for the detection of various gases such as O₂ [69], H₂ [70], ammonia [71], as well as volatile organic compounds [72], while β -Ga₂S₃ has been used for detection of NO₂ [31] and O₂ [73]. However, the sensing properties of a β -Ga₂O₃- β -Ga₂S₃ composite have not yet been investigated.

β -Ga₂O₃- β -Ga₂S₃ is composed of the semiconductor materials Ga₂O₃ and Ga₂S₃ with band gap widths of 4.9 eV and 3.1 eV, respectively. β -Ga₂O₃ is a *n*-type semiconductor with an electron concentration of 10¹⁷-10¹⁸ cm⁻³ and a mobility of 40-80 cm²/v·s [32]. While β -Ga₂S₃ is a *p*-type semiconductor [31]. The obtained composite structure is therefore a *p-n* junction.

As already mentioned in the previous section, β -Ga₂S₃ and β -Ga₂O₃ compounds crystallize in monoclinic networks, which is a favourable condition for heterojunctions. Considering the band gap width, Ga₂O₃ and Ga₂S₃ are both classified as materials for functional optoelectronic devices in the UV range [33]. The bandwidth of β -Ga₂O₃, which is 4.9 eV in single crystals and 4.7 ÷ 4.9 eV in nano- and microformations, is greater than that of GaN and SiC semiconductors, making this material attractive for UV optoelectronics, in particular as radiation receptors and sources. The maximum photosensitivity of the receptors is predicted to be at wavelengths shorter than the threshold wavelength (280 nm). Micro- and nanocrystallites present on the surface of the Ga₂O₃ layer contribute to a diffusion of the incident light which leads to an increase

of the absorption rate allowing thus to reduce the thickness of the Ga₂O₃ layer, in which the generation of unbalanced charge carriers takes place. By decreasing the Ga₂O₃ layer thickness, the efficiency of photovoltaic cells based on such junctions can be increased. This makes the β -Ga₂O₃- β -Ga₂S₃ composite highly attractive for sensing applications. Therefore, we are planning to fabricate UV photodetectors and gas sensing devices based on the synthesized β -Ga₂O₃- β -Ga₂S₃ to demonstrate the practical application potential.

4. Conclusions

In this work, homogenous nanostructured layers of β -Ga₂O₃ were obtained on a Ga₂S₃ substrate by thermal annealing in air of β -Ga₂S₃ single crystals grown using the CVD method. The influence of the annealing temperature (970-1170 K) on morphological, compositional, structural and optical characteristics of β -Ga₂O₃- β -Ga₂S₃ composites was investigated in detail. It has been shown by means of Raman spectroscopy, EDX spectroscopy and diffusive reflection spectra that the surface of Ga₂S₃ single crystals thermally annealed at temperatures of 1070 K and 1170 K under normal ambient conditions is covered with a homogeneous layer of β -Ga₂O₃ oxide. XRD diffractograms confirm that after thermal annealing of Ga₂S₃ monocrystals at the temperature of 1073 K, the surface is composed of β -Ga₂O₃ and β -Ga₂S₃ crystallites with submicrometric dimensions which can be clearly seen in SEM. The spectrum of the oxide on the surface of the single crystal Ga₂S₃ is composed of micro and nanocrystallites that diffuse the incident light. Initially, nano-islands of β -Ga₂O₃ nanostructures are formed on the surface, which are then transformed with the increase of the annealing temperature into a homogeneous micro- and nano-granulated layer that diffuses the incident light. Optical measurements of the β -Ga₂O₃ nanostructures demonstrated the direct bandgap optical transitions. By increasing the annealing temperature from 970 K to 1170 K the decrease in bandgap value from 4.41 eV to 4.3 eV was observed. The β -Ga₂O₃ oxide layer is a photoluminescent material in the blue region of the spectrum. It was observed that the maximum of the photoluminescence band moves slowly to long wavelengths with the increase of the annealing temperature from 970 K to 1170 K. Reported data are important for fundamental research and for development of new devices, especially sensors for harsh environments.

Author statement

The manuscript was written through contributions of all authors. All authors have given approval to the final version of the manuscript. V.S., I.C., L.P. and M.C. synthesized the nanomaterial. V.S. and M.C. adapted procedure for thermal treatment of nanomaterial. O.L., V.P., M.C. and R. A. realized Raman experiments and data analysis. O.L. and V.P. adapted technological approach for material integration/fabrication of the sensors, carried out the measurement of sensing properties, not included here. A.C. and A.G. did SEM-EDX studies. V.S., D.U. and O.L. realized XRD experiments and data analysis. V.S. and M.C. realized all PL experiments and data analysis. V.S., I.C., D.U. and M.C. realized all optical experiments and data analysis. O.L., V.S., R.A., and I.T. analyzed the results, including experimental data and revised draft. O.L., V.S., V.P., I. T., A.G. and M.C. drafting the article. V.S., M.C., O.L., R.A. and I.C. study conception and design, final approval of the version to be published. All authors reviewed the manuscript.

Declaration of competing interest

The authors declare that they have no known competing financial interests or personal relationships that could have appeared to influence the work reported in this paper.

Acknowledgements

This work was financially supported by Moldova State University through the Institutional Grant No. 15.817.02.34A, the Estonian Ministry of Education and Research (IUT19-4), as well as the European Regional Development Fund [project TK141: Centre of Excellence ‘Advanced materials and high-technology devices for sustainable energetics, sensorics and nano-electronics’ (1.01.2015–1.03.2023)]. Dr. Lupan acknowledges the Alexander von Humboldt Foundation for the research fellowship for experienced researchers (3-3MOL/1148833 STP) at the Institute for Materials Science, Kiel University, Germany. Katrin Brandenburg is acknowledged for her help in the final proof-reading of the manuscript. This work was partially supported by the European Commission under the Grant #810652 ‘NanoMedTwin. This work was partially supported by the Technical University of Moldova and through the ANCD-NARD Grant No. 20.80009.5007.09 at TUM.

Appendix A. Supplementary data

Supplementary data to this article can be found online at <https://doi.org/10.1016/j.mssp.2020.105314>.

References

- M. Higashiwaki, K. Sasaki, A. Kuramata, T. Masui, S. Yamakoshi, Gallium oxide (Ga_2O_3) metal-semiconductor field-effect transistors on single-crystal $\beta\text{-Ga}_2\text{O}_3$ (010) substrates, *Appl. Phys. Lett.* 100 (2012), 013504.
- M. Zhong, Z. Wei, X. Meng, F. Wu, J. Li, High-performance single crystalline UV photodetectors of $\beta\text{-Ga}_2\text{O}_3$, *J. Alloys Compd.* 619 (2015) 572–575.
- M. Higashiwaki, K. Sasaki, H. Murakami, Y. Kumagai, A. Koukita, A. Kuramata, T. Masui, S. Yamakoshi, Recent progress in Ga_2O_3 power devices, *Semicond. Sci. Technol.* 31 (2016), 034001.
- H.F. Liu, K.K.A. Antwi, N.L. Yakovlev, H.R. Tan, L.T. Ong, S.J. Chua, D.Z. Chi, Synthesis and phase evolutions in layered structure of Ga_2S_3 semiconductor thin films on epi-ready GaAs (111) substrates, *ACS Appl. Mater. Interfaces* 6 (2014) 3501–3507.
- R. Zou, Z. Zhang, Q. Liu, J. Hu, L. Sang, M. Liao, W. Zhang, High detectivity solar-blind high-temperature deep-ultraviolet photodetector based on multi-layered (100) facet-oriented $\beta\text{-Ga}_2\text{O}_3$ nanobelts, *Small* 10 (2014) 1848–1856.
- B. Zhao, F. Wang, H. Chen, L. Zheng, L. Su, D. Zhao, X. Fang, An ultrahigh responsivity (9.7 mA W^{-1}) self-powered solar-blind photodetector based on individual $\text{ZnO-Ga}_2\text{O}_3$ heterostructures, *Adv. Funct. Mater.* 27 (2017), 1700264.
- Y. Li, T. Tokizono, M. Liao, M. Zhong, Y. Koide, I. Yamada, J.-J. Delaunay, Efficient assembly of bridged $\beta\text{-Ga}_2\text{O}_3$ nanowires for solar-blind photodetection, *Adv. Funct. Mater.* 20 (2010) 3972–3978.
- X. Zhang, L. Wang, X. Wang, Y. Chen, Q. Shao, G. Wu, X. Wang, T. Lin, H. Shen, J. Wang, High-performance $\beta\text{-Ga}_2\text{O}_3$ thickness dependent solar blind photodetector, *Optic Express* 28 (2020) 4169–4177.
- S. Kumar, R. Singh, Nanofunctional gallium oxide (Ga_2O_3) nanowires/nanostructures and their applications in nanodevices, *Phys Status Solidi RRL* 7 (2013) 781–792.
- Y.M. Juan, S.J. Chang, H.T. Hsueh, T.C. Chen, S.W. Huang, Y.H. Lee, T.J. Hsueh, C. L. Wu, Self-powered hybrid humidity sensor and dual-band UV photodetector fabricated on back-contact photovoltaic cell, *Sens. Actuators, B* 219 (2015) 43–49.
- W.-Y. Kong, G.-A. Wu, K.-Y. Wang, T.-F. Zhang, Y.-F. Zou, D.-D. Wang, L.-B. Luo, Graphene- $\beta\text{-Ga}_2\text{O}_3$ heterojunction for highly sensitive deep UV photodetector application, *Adv. Mater.* 28 (2016) 10725–10731.
- M. Chen, B. Zhao, G. Hu, X. Fang, H. Wang, L. Wang, J. Luo, X. Han, X. Wang, C. Pan, Z.L. Wang, Piezo-phototronic effect modulated deep UV photodetector based on $\text{ZnO-Ga}_2\text{O}_3$ heterojunction microwire, *Adv. Funct. Mater.* 28 (2018), 1706379.
- C. Baban, Y. Toyoda, M. Ogita, Oxygen sensing at high temperatures using Ga_2O_3 films, *Thin Solid Films* 484 (2005) 369–373.
- M. Fleischer, H. Meixner, Gallium oxide thin films: a new material for high-temperature oxygen sensors, *Sens. Actuators, B* 4 (1991) 437–441.
- A. Afzal, $\beta\text{-Ga}_2\text{O}_3$ nanowires and thin films for metal oxide semiconductor gas sensors: sensing mechanisms and performance enhancement strategies, *J. Materiomics* 5 (2019) 542–557.
- L. Li, E. Auer, M. Liao, X. Fang, T. Zhai, U.K. Gautam, A. Lugstein, Y. Koide, Y. Bando, D. Golberg, Deep-ultraviolet solar-blind photoconductivity of individual gallium oxide nanobelts, *Nanoscale* 3 (2011) 1120–1126.
- O. Lupan, T. Braniste, M. Deng, L. Ghimpu, I. Paulowicz, Y.K. Mishra, L. Kienle, R. Adelung, I. Tiginyanu, Rapid switching and ultra-responsive nanosensors based on individual shell-core $\text{Ga}_2\text{O}_3/\text{GaN:O}_x/\text{SnO}_2$ nanobelt with nanocrystalline shell in mixed phases, *Sens. Actuators, B* 221 (2015) 544–555.
- J.-S. Hwang, T.-Y. Liu, S. Chattopadhyay, G.-M. Hsu, A.M. Basilio, H.-W. Chen, Y.-K. Hsu, W.-H. Tu, Y.-G. Lin, K.-H. Chen, C.-C. Li, S.-B. Wang, H.-Y. Chen, L.-C. Chen, Growth of $\beta\text{-Ga}_2\text{O}_3$ and GaN nanowires on GaN for photoelectrochemical hydrogen generation, *Nanotechnology* 24 (2013), 055401.
- B. Fu, Z. Jia, W. Mu, Y. Yin, J. Zhang, X. Tao, A review of $\beta\text{-Ga}_2\text{O}_3$ single crystal defects, their effects on device performance and their formation mechanism, *J. Semiconduct.* 40 (2019), 011804.
- A. Mirzaei, G. Neri, Microwave-assisted synthesis of metal oxide nanostructures for gas sensing application: a review, *Sens. Actuators, B* 237 (2016) 749–775.
- V.M. Bermudez, S.M. Prokes, Infrared spectroscopy and surface chemistry of $\beta\text{-Ga}_2\text{O}_3$ nanoribbons, *Langmuir* 23 (2007) 12566–12576.
- K.F. Cai, S. Shen, C. Yan, S. Bateman, Preparation, characterization and formation mechanism of gallium oxide nanowires, *Curr. Appl. Phys.* 8 (2008) 363–366.
- E. Filippo, M. Siciliano, A. Genga, G. Micocci, A. Tepore, T. Siciliano, Single crystalline $\beta\text{-Ga}_2\text{O}_3$ nanowires synthesized by thermal oxidation of GaSe layer, *Mater. Res. Bull.* 48 (2013) 1741–1744.
- B.C. Kim, K.T. Sun, K.S. Park, K.J. Im, T. Noh, M.Y. Sung, S. Kim, S. Nahm, Y. N. Choi, S.S. Park, $\beta\text{-Ga}_2\text{O}_3$ nanowires synthesized from milled GaN powders, *Appl. Phys. Lett.* 80 (2002) 479–481.
- L. Leontie, V. Sprincean, D. Untila, N. Spalatu, I. Caraman, A. Cojocaru, O. Şuşu, O. Lupan, I. Evtodiev, E. Vatavu, I. Tiginyanu, A. Carlescu, M. Caraman, Synthesis and optical properties of Ga_2O_3 nanowires grown on GaS substrate, *Thin Solid Films* 689 (2019), 137502.
- H.P. Ho, K.C. Lo, K.Y. Fu, P.K. Chu, K.F. Li, K.W. Cheah, Synthesis of beta gallium oxide nano-ribbons from gallium arsenide by plasma immersion ion implantation and rapid thermal annealing, *Chem. Phys. Lett.* 382 (2003) 573–577.
- Y. Bayam, V.J. Logeeswaran, A.M. Katzenmeyer, R.J. Chacon, M.C. Wong, C. E. Hunt, M.S. Islam, Synthesis and field emission characteristics of Ga_2O_3 nanorods with ultra-sharp tips, in: 2008 8th IEEE Conference on Nanotechnology, 2008, pp. 573–575.
- E. Filippo, M. Tepore, F. Baldassarre, T. Siciliano, G. Micocci, G. Quarta, L. Calcagnile, A. Tepore, Synthesis of $\beta\text{-Ga}_2\text{O}_3$ microstructures with efficient photocatalytic activity by annealing of GaSe single crystal, *Appl. Surf. Sci.* 338 (2015) 69–74.
- E. Filippo, T. Siciliano, A. Genga, G. Micocci, M. Siciliano, A. Tepore, Phase and morphological transformations of GaS single crystal surface by thermal treatment, *Appl. Surf. Sci.* 261 (2012) 454–457.
- S.J. Pearton, J. Yang, P.H. Cary, F. Ren, J. Kim, M.J. Tadjer, M.A. Mastro, A review of Ga_2O_3 materials, processing, and devices, *Appl. Phys. Rev.* 5 (2018), 011301.
- M.M.Y.A. Alsaif, N. Pillai, S. Kuriakose, S. Walia, A. Jannat, K. Xu, T. Alkathiri, M. Mohiuddin, T. Daeneke, K. Kalantar-Zadeh, J.Z. Ou, A. Zavabeti, Atomically thin Ga_2S_3 from skin of liquid metals for electrical, optical, and sensing applications, *ACS Appl. Nano Mater.* 2 (2019) 4665–4672.
- M. Orita, H. Ohta, M. Hirano, H. Hosono, Deep-ultraviolet transparent conductive $\beta\text{-Ga}_2\text{O}_3$ thin films, *Appl. Phys. Lett.* 77 (2000) 4166–4168.
- D.R. Miller, S.A. Akbar, P.A. Morris, Nanoscale metal oxide-based heterojunctions for gas sensing: a review, *Sens. Actuators, B* 204 (2014) 250–272.
- J. Gröttrup, V. Postica, D. Smazna, M. Hoppe, V. Kaidas, Y.K. Mishra, O. Lupan, R. Adelung, UV detection properties of hybrid ZnO tetrapod 3-D networks, *Vacuum* 146 (2017) 492–500.
- K.A. Kokh, B.G. Nenashev, A.E. Kokh, G.Y. Shvedenkov, Application of a rotating heat field in Bridgman–Stockbarger crystal growth, *J. Cryst. Growth* 275 (2005) e2129–e2134.
- R. Honig, D. Kramer, Vapor Pressure Curves of the Elements, RCA Laboratories, 1968.
- O. Lupan, V. Postica, V. Cretu, N. Wolff, V. Duppel, L. Kienle, R. Adelung, Single and networked CuO nanowires for highly sensitive p-type semiconductor gas sensor applications, *Phys Status Solidi RRL* 10 (2016) 260–266.
- L. Siebert, N. Wolff, N. Ababii, M.-I. Terasa, O. Lupan, A. Vahl, V. Duppel, H. Qiu, M. Tienken, M. Mirabelli, V. Sontea, F. Faupel, L. Kienle, R. Adelung, Facile fabrication of semiconducting oxide nanostructures by direct ink writing of readily available metal microparticles and their application as low power acetone gas sensors, *Nano Energy* 70 (2020), 104420.
- K. Girija, S. Thirumalairajan, G.S. Avadhani, D. Mangalaraj, N. Ponpandian, C. Viswanathan, Synthesis, morphology, optical and photocatalytic performance of nanostructured $\beta\text{-Ga}_2\text{O}_3$, *Mater. Res. Bull.* 48 (2013) 2296–2303.
- S.I. Boldish, W.B. White, Optical band gaps of selected ternary sulfide minerals, *Am. Mineral.* 83 (1998) 865–871.
- A.P. Vel'muzhov, M.V. Sukhanov, A.M. Potapov, A.I. Suchkov, M.F. Churbanov, Preparation of extrapure Ga_2S_3 by reacting GaI_3 with sulfur, *Inorg. Mater.* 50 (2014) 656–660.
- Y. Zhang, C. Chen, C.Y. Liang, Z.W. Liu, Y.S. Li, R. Che, Strain-tuned optoelectronic properties of hollow gallium sulphide microspheres, *Nanoscale* 7 (2015) 17381–17386.
- B.D. Cullity, Elements of X-Ray Diffraction, Addison-Wesley Publishing, 1956.
- R. Roy, V.G. Hill, E.F. Osborn, Polymorphism of Ga_2O_3 and the system $\text{Ga}_2\text{O}_3\text{-H}_2\text{O}$, *J. Am. Chem. Soc.* 74 (1952) 719–722.
- S.E. Collins, M.A. Baltanás, A.L. Bonivardi, Hydrogen chemisorption on gallium oxide polymorphs, *Langmuir* 21 (2005) 962–970.
- H. Peelaers, C.G. Van de Walle, Brillouin zone and band structure of $\beta\text{-Ga}_2\text{O}_3$, *Phys. Status Solidi* 252 (2015) 828–832.
- C. Galván, M. Galván, J.S. Arias-Cerón, E. López-Luna, H. Vilchis, V.M. Sánchez-R, Structural and Raman studies of Ga_2O_3 obtained on GaAs substrate, *Mater. Sci. Semicond. Process.* 41 (2016) 513–518.
- I.E. Wachs, Raman and IR studies of surface metal oxide species on oxide supports: supported metal oxide catalysts, *Catal. Today* 27 (1996) 437–455.
- V. Postica, A. Vahl, D. Santos-Carballal, T. Dankwort, L. Kienle, M. Hoppe, A. Cadi-Essadek, N.H. de Leeuw, M.-I. Terasa, R. Adelung, F. Faupel, O. Lupan, Tuning ZnO sensors reactivity toward volatile organic compounds via Ag doping and

- nanoparticle functionalization, *ACS Appl. Mater. Interfaces* 11 (2019) 31452–31466.
- [50] V. Postica, A. Vahl, J. Strobel, D. Santos-Carballal, O. Lupan, A. Cadi-Essadek, N. H. de Leeuw, F. Schütt, O. Polonskyi, T. Strunskus, M. Baum, L. Kienle, R. Adelung, F. Faupel, Tuning doping and surface functionalization of columnar oxide films for volatile organic compound sensing: experiments and theory, *J. Mater. Chem.* 6 (2018) 23669–23682.
- [51] D. Machon, P.F. McMillan, B. Xu, J. Dong, High-pressure study of the β -to- α transition in Ga_2O_3 , *Phys. Rev. B* 73 (2006), 094125.
- [52] C. Kranert, C. Sturm, R. Schmidt-Grund, M. Grundmann, Raman tensor elements of β - Ga_2O_3 , *Sci. Rep.* 6 (2016), 35964.
- [53] T. Onuma, S. Fujioka, T. Yamaguchi, Y. Itoh, M. Higashiwaki, K. Sasaki, T. Masui, T. Honda, Polarized Raman spectra in β - Ga_2O_3 single crystals, *J. Cryst. Growth* 401 (2014) 330–333.
- [54] D. Dohy, G. Lucazeau, A. Revcolevschi, Raman spectra and valence force field of single-crystalline β Ga_2O_3 , *J. Solid State Chem.* 45 (1982) 180–192.
- [55] J. Li, X. Chen, Z. Qiao, M. He, H. Li, Large-scale synthesis of single-crystalline β - Ga_2O_3 nanoribbons, nanosheets and nanowires, *J. Phys. Condens. Matter* 13 (2001) L937–L941.
- [56] V.I. Nikolaev, A.I. Pechnikov, S.I. Stepanov, I.P. Nikitina, A.N. Smirnov, A. V. Chikiryaka, S.S. Sharofidinov, V.E. Bougrov, A.E. Romanov, Epitaxial growth of (2 01) β - Ga_2O_3 on (0001) sapphire substrates by halide vapour phase epitaxy, *Mater. Sci. Semicond. Process.* 47 (2016) 16–19.
- [57] J.Q. Ning, S.J. Xu, P.W. Wang, Y.P. Song, D.P. Yu, Y.Y. Shan, S.T. Lee, H. Yang, Microstructure and micro-Raman studies of nitridation and structure transition of gallium oxide nanowires, *Mater. Char.* 73 (2012) 153–157.
- [58] Y. Zhu, Q.-K. Yu, G.-Q. Ding, X.-G. Xu, T.-R. Wu, Q. Gong, N.-Y. Yuan, J.-N. Ding, S.-M. Wang, X.-M. Xie, M.-H. Jiang, Raman enhancement by graphene- Ga_2O_3 2D bilayer film, *Nanoscale Res Lett* 9 (2014) 48.
- [59] Y. Li, L. You, R. Duan, P. Shi, G. Qin, Oxidation of a ZnS nanobelt into a ZnO nanotwin belt or double single-crystalline ZnO nanobelts, *Solid State Commun.* 129 (2004) 233–238.
- [60] B. Liu, M. Gu, X. Liu, Lattice dynamical, dielectric, and thermodynamic properties of β - Ga_2O_3 from first principles, *Appl. Phys. Lett.* 91 (2007), 172102.
- [61] Y.C. Choi, W.S. Kim, Y.S. Park, S.M. Lee, D.J. Bae, Y.H. Lee, G.S. Park, W.B. Choi, N.S. Lee, J.M. Kim, Catalytic growth of β - Ga_2O_3 nanowires by arc discharge, *Adv. Mater.* 12 (2000) 746–750.
- [62] X. Du, Z. Li, C. Luan, W. Wang, M. Wang, X. Feng, H. Xiao, J. Ma, Preparation and characterization of Sn-doped β - Ga_2O_3 homoepitaxial films by MOCVD, *J. Mater. Sci.* 50 (2015) 3252–3257.
- [63] Z. Chen, X. Wang, S. Noda, K. Saito, T. Tanaka, M. Nishio, M. Arita, Q. Guo, Effects of dopant contents on structural, morphological and optical properties of Er doped Ga_2O_3 films, *Superlattice. Microst.* 90 (2016) 207–214.
- [64] M. Muruganandham, R. Amutha, M.S.M.A. Wahed, B. Ahmmad, Y. Kuroda, R.P. S. Suri, J.J. Wu, M.E.T. Sillanpää, Controlled fabrication of α - GaOOH and α - Ga_2O_3 self-assembly and its superior photocatalytic activity, *J. Phys. Chem. C* 116 (2012) 44–53.
- [65] S. Kumar, C. Tessarek, S. Christiansen, R. Singh, A comparative study of β - Ga_2O_3 nanowires grown on different substrates using CVD technique, *J. Alloys Compd.* 587 (2014) 812–818.
- [66] Y. Hou, L. Wu, X. Wang, Z. Ding, Z. Li, X. Fu, Photocatalytic performance of α -, β -, and γ - Ga_2O_3 for the destruction of volatile aromatic pollutants in air, *J. Catal.* 250 (2007) 12–18.
- [67] L. Dai, X.L. Chen, X.N. Zhang, A.Z. Jin, T. Zhou, B.Q. Hu, Z. Zhang, Growth and optical characterization of Ga_2O_3 nanobelts and nanosheets, *J. Appl. Phys.* 92 (2002) 1062–1064.
- [68] K.M. Othonos, M. Zervos, C. Christofides, A. Othonos, Ultrafast spectroscopy and red emission from β - Ga_2O_3 / β - Ga_2S_3 nanowires, *Nanoscale Res Lett* 10 (2015) 304.
- [69] M. Ogita, K. Higo, Y. Nakanishi, Y. Hatanaka, Ga_2O_3 thin film for oxygen sensor at high temperature, *Appl. Surf. Sci.* 175–176 (2001) 721–725.
- [70] S. Nakagomi, T. Sai, Y. Kokubun, Hydrogen gas sensor with self temperature compensation based on β - Ga_2O_3 thin film, *Sens. Actuators, B* 187 (2013) 413–419.
- [71] R. Pandeewari, B.G. Jeyaprakash, High sensing response of β - Ga_2O_3 thin film towards ammonia vapours: influencing factors at room temperature, *Sens. Actuators, B* 195 (2014) 206–214.
- [72] S. Stegmeier, M. Fleischer, P. Hauptmann, Influence of the morphology of platinum combined with β - Ga_2O_3 on the VOC response of work function type sensors, *Sens. Actuators, B* 148 (2010) 439–449.
- [73] C.-H. Ho, M.-H. Lin, Y.-P. Wang, Y.-S. Huang, Synthesis of In_2S_3 and Ga_2S_3 crystals for oxygen sensing and UV photodetection, *Sens. Actuators, A* 245 (2016) 119–126.